Analyst

PAPER

Label-free colorimetric sensing of cobalt(II) based on inducing aggregation of thiosulfate stabilized gold nanoparticles in the presence of ethylenediamine

Zhiyang Zhang,[ac] Jun Zhang,[b] Tingting Lou,[ac] Dawei Pan,[a] Lingxin Chen,[a] Chengli Qu[a] and Zhaopeng Chen*[a]

As a sensitive and selective analytical technique, gold nanoparticles-based colorimetric sensing was characterized by its simplicity and cost-effectiveness. Specific methods have been extensively developed for different targets in diverse samples. In this study, a label-free method for sensing Co^{2+} in aqueous solutions was described. The target was achieved by the induced aggregation of thiosulfate ($S_2O_3^{2-}$) stabilized gold nanoparticles (AuNPs) in the presence of ethylenediamine (en). Co^{2+} first reacted with en and formed complexes of $Co(en)_3^{2+}$ in aqueous solutions, which was followed by the oxidation of $Co(en)_3^{2+}$ to $Co(en)_3^{3+}$ by dissolved oxygen. $Co(en)_3^{3+}$ then attacked $S_2O_3^{2-}$ ligands adsorbed on the AuNPs' surfaces, forming positively charged $(en)_2CoS_2O_3^+$ on the AuNPs' surfaces, which reduced the surface charges of AuNPs and induced the aggregation of AuNPs. The process was accompanied by a red-shift in the adsorption spectrum and a visible colour change from wine red to blue. Potential effects of relevant experimental conditions, including pH, concentrations of $S_2O_3^{2-}$ and en, and incubation time were evaluated for optimization of the method. The proposed method is sensitive (LOD = 0.0 4 µM or 2.36 ppb) and selective (by at least 100-fold over other metal ions except for Cu^{2+}) toward Co^{2+} with a linear range from 0.1 to 0.7 µM. The cost-effective method allows rapid and simple determination of the concentrations of Co^{2+} ions in drinking water.

Introduction

For decades, the precise determination of heavy metals has been arousing growing interests with respect to environmental problems. Cobalt, as a biologically essential element, used to be barely concerned in environmental researches. However, it was reported that the increase of serum cobalt concentrations was probably associated with certain diseases. Cobalt and some of its compounds were suggested to be potential etiological toxins and likely present carcinogenic effects.[1] On the other hand, cobalt is steadily getting enriched in the surficial environment with the rapid development of metallurgy. All these result in the urgency to re-evaluate the pollutive possibility of cobalt.

The abundance of cobalt in environmental samples is generally present at trace levels, which was traditionally determined by voltammetry,[2-7] atomic absorption spectrometry (AAS),[8-10] inductively coupled plasma mass spectrometry (ICP-MS),[11,12] *etc.* AAS and ICP-MS are either time consuming or relatively high-cost. Their application in field tests and on-site monitoring thereby is very limited. Voltammetry is a convenient, quick and sensitive method. Unfortunately, this method usually uses noxious mercury film electrodes or chemical modified electrodes which need cumbersome modification progress. As an easily operated and cost effective instrument, spectrophotometry has proven to be practical in the determination of cobalt in natural waters.[13-15] The major disadvantage of these methods is the relatively higher detection limits resulting from low photo-absorption coefficients of the Co-organic complex.

Metal nanoparticles, especially gold nanoparticles (AuNPs), are now widely employed in biological and biomedical applications.[16-22] Because of their unique size-dependent optical and electronic properties, AuNPs are particularly concerned in colorimetric assays of heavy metal ions (*e.g.* Pb^{2+},[23-25] Cu^{2+},[26] Hg^{2+},[27-29] and Cr^{3+}).[30] It should be noted that the above results were achieved *via* labeled AuNPs, *i.e.* using the formation of ion-ligand complexes to induce aggregation of AuNPs. Such methods need complicated modifying processes (*i.e.* label processes) as well as specific equipments (*e.g.* high speed centrifuges). As a comparison, AuNPs-based label-free colorimetric assays, which take advantage of metal ions themselves to induce the aggregation of AuNPs or improve the leaching of AuNPs, are much simpler and even more economical. Satisfactory results have been achieved in the determination of certain metal ions, *e.g.* Ag^+, Hg^{2+} and Pb^{2+}.[31-33]

[a]Key Laboratory of Coastal Environmental Processes, Yantai Institute of Coastal Zone Research, Chinese Academy of Sciences, Yantai, 264003, China. E-mail: zhpchen@yic.ac.cn; Fax: +86 535 2109133; Tel: +86 535 2109133
[b]School of Tropical and Laboratory Medicine, Hainan Medical University, Haikou, 571101, China
[c]Graduate University of Chinese Academy of Sciences, Beijing, 100049, China

In this study, a label-free AuNPs-based colorimetric method was developed for the rapid sensing of Co^{2+} in aqueous solutions at room temperature. Experiments were conducted *via* $S_2O_3^{2-}$ stabilized AuNPs with the presence of ethylenediamine (en, 0.005% v/v). The principal is briefly described as follows: 1) Co^{2+} reacted with en and formed $Co(en)_3^{2+}$; 2) $Co(en)_3^{2+}$ was oxidized to $Co(en)_3^{3+}$ by dissolved oxygen in aqueous solutions; 3) $Co(en)_3^{3+}$ reacted with $S_2O_3^{2-}$ absorbed on AuNPs and formed a positively charged ion of $(en)_2CoS_2O_3^{+}$. As a final result, AuNPs were aggregated and the colour of aqueous solutions changed from wine red to dark blue. Further tests proved that the above method was applicable to the rapid determination of Co^{2+} in drinking water.

Experimental

Chemicals and apparatus

Hydrogen tetrachloroaurate(III) dehydrate, trisodium citrate, ethylenediamine, sodium thiosulfate and glycin were obtained from Sinopharm Chemical Reagent (China). All other chemicals were analytical reagent grade or better. Solutions were prepared with deionized water (18.2 MΩ, Pall® Cascada). Absorption spectra of AuNPs were scanned by UV/visible spectrophotometer (Beckman Coulter® DU-800, USA). Images of dispersed AuNPs were achieved by transmission electron microscopy (TEM, JEOL® JEM-1230, Japan) operated at 100 kV. Dynamic light scattering (DLS) experiments were performed on a Zeta Potential/Particle Sizer (Nicomp® 380 ZLS, USA).

Gold nanoparticles synthesis

Citrate-capped gold nanoparticles were prepared according to Frens' method by means of the chemical reduction of $HAuCl_4$ in the liquid phase.[34] Briefly, 200 mL aqueous solution of 1 mM $HAuCl_4$ was first brought to boil with vigorous stirring in a round bottom flask equipped with a reflux condenser. Then 38.8 mM trisodium citrate (20 mL) was added rapidly and the mixture was heated under reflux for another 15 min. During this process, the colour changed from pale yellow to deep red. Thereafter, the solution was cooled to room temperature while being stirred continuously. The size of AuNPs, as determined by TEM imaging, was ~13 nm. The particle concentration of the gold nanoparticles (*ca.* 15 nM) was determined according to Beer's law using an extinction coefficient of *ca.* 2.43×10^8 M^{-1} cm^{-1} at 520 nm.

Sensing procedure

300 μL AuNPs (15 nM, the use of 300 μL AuNPs could achieve highest sensitivity, the effect of the concentration of AuNPs was not shown) was added to 710 μL 0.1 M glycine-NaOH buffers, while either $S_2O_3^{2-}$ or Co^{2+} in buffers were set at different levels. The mixed solutions were incubated for 2 min to stabilize the AuNPs. Thereafter 5.0 μL of en with different concentrations was added to the mixture. Equilibrated at room temperature for different intervals, the final solutions were scanned to record the adsorption spectra.

Analysis of practical samples

A series of practical samples were prepared by spiking standard solutions of Co^{2+} to local drinking water. The pH of the samples (630 μL) was adjusted to 9.0 by the addition of 1.0 M glycine-NaOH buffer solution (70 μL). Thereafter 10 μL $Na_2S_2O_3$ (0.05 M), 300 μL AuNPs and 5.0 μL en (1% v/v) were sequentially introduced. The final solutions were incubated at room temperature for 20 min before the spectrum scan.

Results and discussion

Sensing mechanism

As shown in Scheme 1, AuNPs were first stabilized by negatively charged $S_2O_3^{2-}$ in glycine-NaOH buffers (pH = 9.0). $S_2O_3^{2-}$ was strongly absorbed to the AuNPs' surface, which ensures that the AuNPs were stable even in solutions with high ionic strength.[32] The absorbed $S_2O_3^{2-}$ also blocked the accession of amino groups of en to the AuNPs' surface and prevented the AuNPs from aggregation. However, when Co^{2+} was added, such a balance would be broken. Co^{2+} first reacted with en to form $Co(en)_3^{2+}$. It is noticeable that $Co(en)_3^{2+}$ can be easily oxidized to $Co(en)_3^{3+}$ by dissolved oxygen,[35] since the ox/red potential of $Co(en)_3^{3+}/Co(en)_3^{2+}$ is -0.2 V and far less than that of O_2/H_2O (0.93 V, calculated according to the Nernst Equation at pH 9.0). Subsequently, $Co(en)_3^{3+}$ in the aqueous solutions reacted with $S_2O_3^{2-}$ on the AuNPs' surface, which formed a positively charged ion, $(en)_2CoS_2O_3^{+}$, on the AuNPs' surface.[36] As a result, the AuNPs became aggregated due to the lack of sufficient surface charges.

To further confirm that these AuNPs aggregated, we compared the DLS data of $S_2O_3^{2-}$ stabilized AuNPs before and after incubation with Co^{2+} in the presence of en, the intensity-weighting Gaussian distribution curves showed the average hydrodynamic diameter of well dispersed AuNPs was 47.9 nm, while that of the Co^{2+}-induced aggregation of AuNPs increases to be 177.5 nm (Fig. 1). It is reasonable to conclude that the aggregation of AuNPs should be attributed to the addition of Co^{2+}. The major reason is probably associated with the 3 lone electron pairs of the S atom of $S_2O_3^{2-}$. Such a characteristic allows $S_2O_3^{2-}$ to be coordinated with Au^+ and get self-assembled onto the AuNPs' surfaces.[32] However, for the single S atom, only one lone electron pair was consumed and the other two still remained accessible for Co(III). Despite the presence of abundant $S_2O_3^{2-}$ in aqueous solutions, $Co(en)_3^{3+}$ ions are presumed to preferentially react with $S_2O_3^{2-}$ ligands adsorbed on the AuNPs' surface and form $(en)_2CoS_2O_3^{+}$. The fact, we think, should be attributed to the much higher electron density on the AuNPs' surface.
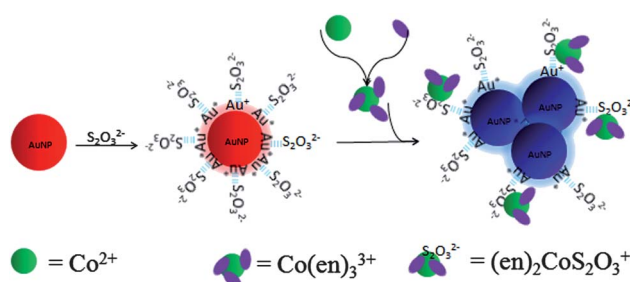
Scheme 1 Mechanism of $S_2O_3^{2-}$ stabilized AuNPs for sensing of Co^{2+}.

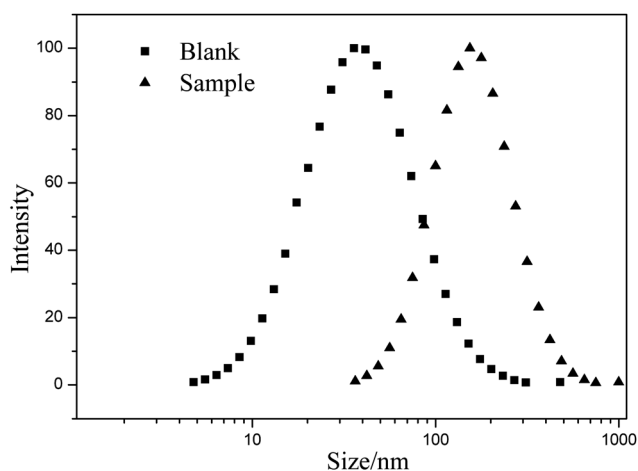**Fig. 1** DLS measurement for $S_2O_3^{2-}$ stabilized AuNPs before (■) and after (▲) incubation with Co^{2+} in the presence of en.

When the AuNPs were well dispersed in aqueous solutions, the initial colloid would appear wine red with a spectral peak around 525 nm (curve a and photographic image A in Fig. 2). The phenomenon was reported to result from the surface plasmon resonance with extremely high extinction coefficients (2.7×10^8 M^{-1} cm^{-1}, >1000 times higher than those of organic dyes).[37] Once the AuNPs got aggregated, a red shift of surface plasmon absorption would occur and be accompanied with a visible colour change from red to blue. It is exactly what was observed in this study, wherein the addition of Co^{2+} caused the maximum absorption wavelength to shift from 525 to around 700 nm and a colour change from red to blue (curve b and photographic image B in Fig. 2).

Optimization of experimental conditions

The colorimetric assay of Co^{2+} was quantitatively conducted *via* the relation between Co^{2+} concentrations and the degree of
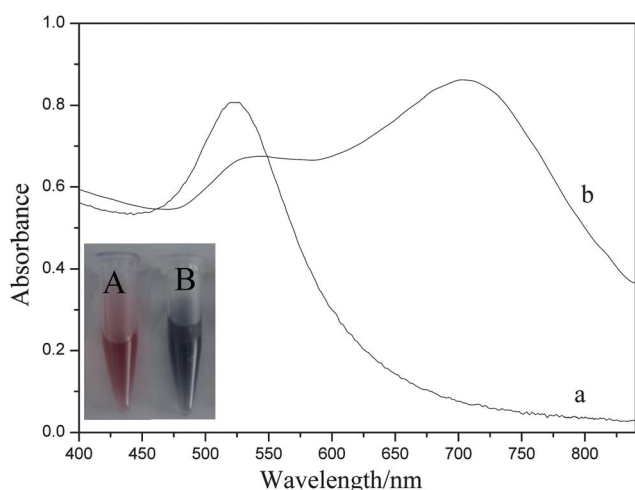
AuNPs aggregation. The latter, to a certain extent, can be quantified by the ratio between adsorption values at 700 nm and those at 525 nm, *i.e.* $A_{700\ nm}/A_{525\ nm}$. It is noteworthy that, more or less, the AuNPs would spontaneously aggregate under any practical conditions. Such spontaneity may even vary with experimental conditions, *e.g.* pH, incubation time, concentrations of $S_2O_3^{2-}$ and en, *etc.* The situation is similar to the Co^{2+} induced aggregation of AuNPs. To minimize such negative effects, it is necessary to optimize the relative experimental conditions as much as possible.

Within the range of 8.6–9.6, the effect of pH was evaluated by the ratio of $(A_{700\ nm}/A_{525\ nm})_{sample}/(A_{700\ nm}/A_{525\ nm})_{blank}$. As shown in Fig. 3, the maximum of calculated ratios was observed around the pH of 9.0. It should be noted that the relative ratios were very sensitive to $(A_{700\ nm}/A_{525\ nm})_{blank}$ instead of $(A_{700\ nm}/A_{525\ nm})_{sample}$. In other words, pH presented much larger negative influence on the spontaneous aggregation of AuNPs. The relative reasons are probably as follows: 1) at lower pH, there was a charge decrease on the AuNPs' surface resulting from protonated en or the decomposition of $S_2O_3^{2-}$; 2) at higher pH, AuNPs became unstable and aggregated to a certain extent before being stabilized by $S_2O_3^{2-}$. In this study, the lowest blank background was found at pH 9.0, so a pH of 9.0 was chosen in following experiments.

In aqueous solutions, $S_2O_3^{2-}$ was introduced to stabilize AuNPs. At low concentrations of $S_2O_3^{2-}$, the AuNPs would aggregate due to the lack of stabilizing agents. On the other hand, high concentrations of $S_2O_3^{2-}$ would cause AuNPs to be continuously oxidized by dissolved oxygen and induce aggregation of the AuNPs.[38] As shown in Fig. 4, the values of $(A_{700\ nm}/A_{525\ nm})_{sample}/(A_{700\ nm}/A_{525\ nm})_{blank}$ first increased sharply with increasing $S_2O_3^{2-}$ concentrations (0 to 0.5 mM) and then gradually decreased. The blank background was minimal when $S_2O_3^{2-}$ was set at 0.5 mM, which remained unaltered in the following experiments.

It should be noted that, without the addition of en, the presence of $S_2O_3^{2-}$ and Co^{2+} was unlikely to induce the aggregation

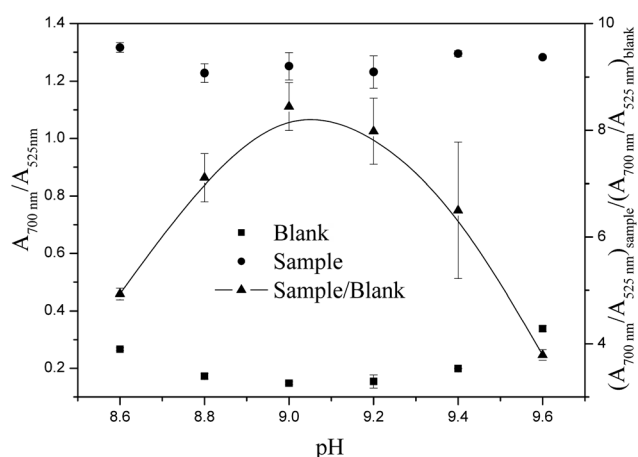**Fig. 2** Absorption spectra and colour (inset) of AuNPs in 70 mM glycine-NaOH buffer solution (pH 9.0) containing 0.5 mM $S_2O_3^{2-}$ and en (0.005%, v/v) in the absence (a, A) and presence (b, B) of Co^{2+} (1.0 μM).

Fig. 3 Effects of pH on the ratios of $(A_{700\ nm}/A_{525\ nm})_{balnk}$ (■), $(A_{700\ nm}/A_{525\ nm})_{sample}$ (●), and $(A_{700\ nm}/A_{525\ nm})_{sample}/(A_{700\ nm}/A_{525\ nm})_{blank}$ (▲). Experimental conditions: 1.0 μM Co^{2+}; $S_2O_3^{2-}$, 0.5 mM; en, 0.01% (v/v); incubation time 20 min.
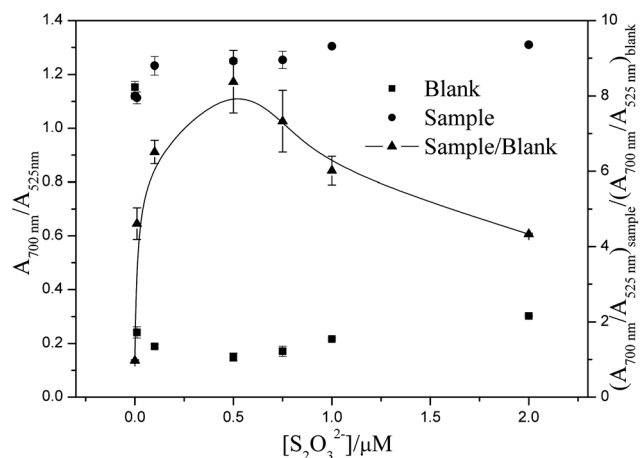
Fig. 4 Effects of $S_2O_3^{2-}$ concentrations on ratios of $(A_{700\ nm}/A_{525\ nm})_{blank}$ (■), $(A_{700\ nm}/A_{525\ nm})_{sample}$ (●), and $(A_{700\ nm}/A_{525\ nm})_{sample}/(A_{700\ nm}/A_{525\ nm})_{blank}$ (▲). Experimental conditions: 1.0 μM Co^{2+}; pH 9.0; en, 0.01% (v/v); incubation time 20 min.

of AuNPs. In this study, the concentration of en was tested from 0 to 0.015% (v/v). As shown in Fig. 5, the value of $(A_{700\ nm}/A_{525\ nm})_{sample}/(A_{700\ nm}/A_{525\ nm})_{blank}$ first increased sharply with en concentrations (0 to 0.005%, v/v), while it would decrease rapidly when en exceeded 0.008% (v/v). AuNPs aggregated slightly at low concentrations of en, since only a few positively charged $(en)_2CoS_2O_3^+$ were formed and absorbed on the AuNPs' surface. However, once the concentration of en exceeded 0.008% (v/v), the AuNPs would partially aggregate due to abundant protonated en in the aqueous solutions. With regard to our results, an en concentration of 0.005% (v/v) was preferred in the following experiments.

Under optimized conditions as mentioned above, AuNPs could keep stable for more than 5 h with the absence of Co^{2+}. Thereafter, the potential effect of the incubation time was evaluated by recording the absorption spectra of a test sample (1.0 μM Co^{2+}). As shown in Fig. 6, the ratio of $A_{700\ nm}/A_{525\ nm}$

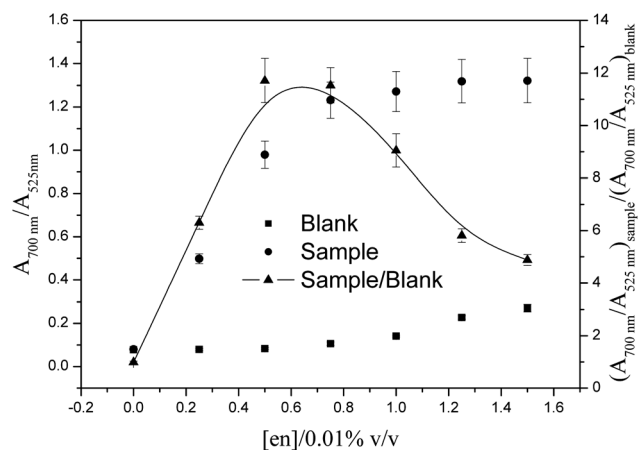**Fig. 5** Effects of en concentrations on ratios of $(A_{700\ nm}/A_{525\ nm})_{blank}$ (■), $(A_{700\ nm}/A_{525\ nm})_{sample}$ (●), and $(A_{700\ nm}/A_{525\ nm})_{sample}/(A_{700\ nm}/A_{525\ nm})_{blank}$ (▲). Experimental conditions: 1.0 μM Co^{2+}; pH 9.0; $S_2O_3^{2-}$, 0.5 mM; incubation time 20 min.
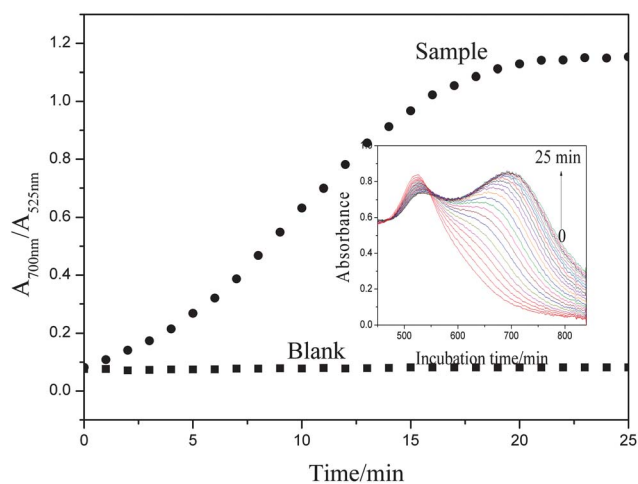

Fig. 6 Effects of the incubation time on ratios of $(A_{700\ nm}/A_{520\ nm})_{sample}$ (●) and $(A_{700\ nm}/A_{520\ nm})_{blank}$ (■). Inset is the absorption spectra at different times with the presence of 1.0 μM Co^{2+}. Other conditions: pH 9.0; $S_2O_3^{2-}$, 0.5 mM; en, 0.005% (v/v).

gradually increased with time before 20 min and then varied slightly. Hence, all the following tests were carried out with an incubation time of 20 min.

Calibration curve, detection limit and selectivity

Since the aggregation of AuNPs would cause a red-shift in the absorption spectrum, the ratio between adsorption values obtained at two given wavelengths was chosen by most researches to represent their results.[23–30] One was the maximum absorption wavelength of aggregated AuNPs (generally around 680 nm) and the other was the maximum absorption wavelength of monodispersed AuNPs (generally around 520 nm). However, such a method sometimes could not accurately represent the degree of AuNPs aggregation. Instead, absorption areas integrated from 525 to 840 nm were chosen in this study as a reference to draw the calibration curve. Standard solutions were prepared by spiking different concentrations of Co^{2+} in glycine-NaOH buffers and thereafter measured under optimized conditions. Their absorbance spectra and colours are shown in Fig. 7. A linear calibration graph was obtained within the range of 0.1–0.7 μM for Co^{2+} (Fig. 7, inset). The detection limit was calculated to be 0.04 μM (2.36 ppb) according to the 3σ-rule (where σ is the standard deviation of a blank solution and $n = 5$).

The detection specificity was also evaluated under the same conditions by adding different metal ions. Corresponding changes in absorption areas and colors are illustrated in Fig. 8. It is obvious that only Co^{2+} could cause significant changes. The excellent selectivity can be expected by comparing stability constants ($\log \beta_2$) of metallic ions with en. In fact, K^+, Mg^{2+}, Ca^{2+}, Pb^{2+}, Fe^{3+}, Cr^{3+} and Al^{3+} cannot form complexes with en, so they can barely induce the aggregation of AuNPs. On the other hand, although Zn^{2+}, Hg^{2+}, Ag^+, Cd^{2+}, Ni^{2+} and Mn^{2+} can form complexes with en, the stability constants with en ($\log \beta_2$, 10.83, 23.3, 7.7, 10.09, 13.8 and 4.79 for Zn^{2+}, Hg^{2+}, Ag^+, Cd^{2+}, Ni^{2+} and Mn^{2+}, respectively) are much less than that of Co^{3+}
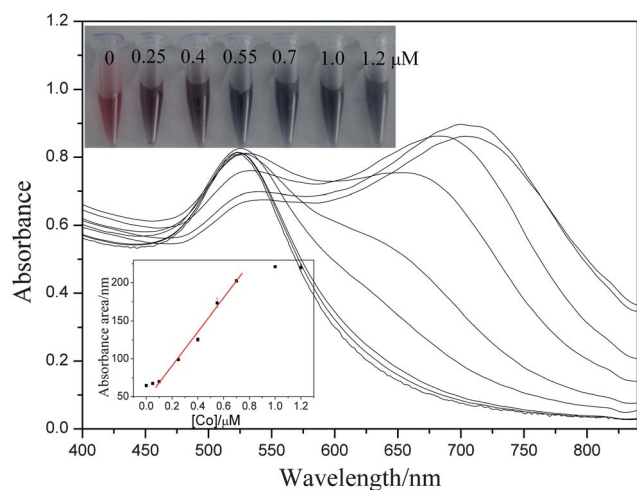
Fig. 7 Absorption spectra of AuNPs in the presence of different concentrations of Co²⁺. Insets are the colour change with the increase of Co²⁺ concentration from left to right and calibration curve, respectively. Conditions: pH 9.0; $S_2O_3^{2-}$, 0.5 mM; en, 0.005%, incubation time 20 min.
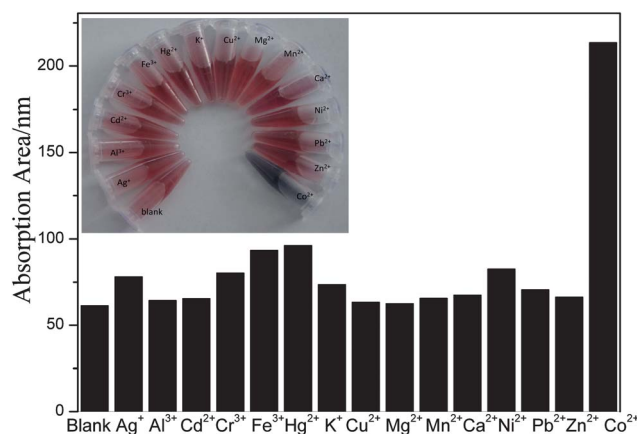

Fig. 8 Adsoption areas and colours (inset) of tested solutions for common metallic ions at 100 μM (besides Cu²⁺, 5.0 μM; Co²⁺, 1.0 μM). Experimental conditions: pH 9.0; $S_2O_3^{2-}$, 0.5 mM; en, 0.005% v/v, incubation time, 20 min.

(*ca.* 34.9). It is noteworthy that, although the log β_2 of Cu(en)$_2^{2+}$ (*ca.* 20.0) is much less than that of Co(en)$_2^{3+}$, 10 μM Cu²⁺ would cause AuNPs aggregation. As what applied in gold mining, the coexistence of $S_2O_3^{2-}$ and Cu²⁺ could accelerate the leaching of AuNPs by dissolved oxygen.[39,40] The metastable state of AuNPs was thereby broken and AuNPs became aggregated.

Analytical application

To evaluate its practical applications, the method was further tested on samples of local drinking water. No Co²⁺ was detected in such samples, which was later verified by ICP-MS. The method was alternatively tested by standard addition and the recovery of spiked Co²⁺ ranged from 92.8 to 110.0% (Table 1). It indicates that such a method is applicable to the quantification of Co²⁺ in aqueous solutions.

Table 1 The recovery of spiked Co²⁺ in local drinking water. The standard deviation of each sample was obtained by three measurements

Sample	Added/μM	Detected/μM	Recovery (%)
Sample	0.25	0.227 ±.02	90.8 ± 8.0
Sample	0.55	0.580 ±.04	105.0 ± 7.3
Sample	0.70	0.770 ±.10	110.0 ± 13

Conclusions

In this study, a sensitive and selective colorimetric method based on inducing aggregation of AuNPs was developed and evaluated for the determination of Co²⁺ in aqueous solutions. The method is highlighted by its simplicity, rapidity and sensitivity compared with many reported colorimetric methods.[14,15,41–44] Such advantages, as well as the practicality validated by analyses of water samples, indicate that the sensing system of Co²⁺ has potential applications in field investigations. What's more, with respect to the fact that the colour change induced by Co²⁺ can be easily observed by the naked eye, the method is expected to be further developed, *e.g.* in the preparation of economical Co²⁺ test-papers.

Acknowledgements

References

1 A. Ensafi, H. R. Mansour and K. Zarei, *Fresenius J. Anal. Chem.*, 1999, **363**, 646.
2 S. Bahrami, S. Abbasi, Y. A. Ghorbani and A. A. Miran-Beigi, *Russ. J. Electrochem.*, 2009, **45**, 208.
3 L. Hosseinzadeh, S. Abbasi, H. Khani and Z. Khani, *Transition Met. Chem.*, 2009, **34**, 425.
4 M. Korolczuk, M. Grabarczyk and A. Moroziewicz, *Electroanalysis*, 2007, **19**, 2155.
5 M. Korolczuk, A. Moroziewicz and M. Grabarczyk, *Anal. Bioanal. Chem.*, 2005, **382**, 1678.
6 K. Tyszczuk, I. Rutyna and M. Korolczuk, *Electroanalysis*, 2009, **21**, 779.
7 M. Vega and C. M. G. van den Berg, *Anal. Chem.*, 1997, **69**, 874.
8 R. S. Praveen, S. Daniel and I. P. Rao, *At. Spectrosc.*, 2006, **27**, 35.
9 K. S. Rao, T. Balaji, T. P. Rao, P. J. Purohit, Y. Babu and G. R. K. Naidu, *Chem. Anal.*, 2004, **49**, 395.
10 A. M. Starvin, V. M. Biju and T. P. Rao, *At. Spectrosc.*, 2004, **25**, 238.
11 M. Fukuda, Y. Hayashibe and Y. Sayama, *Anal. Sci.*, 1995, **11**, 13.
12 E. A. Hutton, J. T. van Elteren, B. I. Ogorevc and M. R. Smyth, *Talanta*, 2004, **63**, 849.
13 H. Eskandari, *Spectrochim. Acta, Part A*, 2006, **63**, 391.
14 N. Shokoufi, F. Shemirani and E. Memarzadeh, *Anal. Chim. Acta*, 2007, **601**, 204.
15 J. Perez-Iglesias, H. Seco-Lago, J. Fernandez-Solis, J. Castro-Romero and V. Gonzalez-Rodriguez, *Ann. Chim.*, 1998, **88**, 597.
16 W. Chen, T. Li, S. He, D. Liu, Z. Wang, W. Zhang and X. Jiang, *Sci. China Chem.*, 2011, **54**, 1227.
17 E. Hutter and D. Maysinger, *Microsc. Res. Tech.*, 2011, **74**, 592.
18 P. F. Jiao, H. Y. Zhou, L. X. Chen and B. Yan, *Curr. Med. Chem.*, 2011, **18**, 2086.

19 Z.-Z. J. Lim, J.-E. J. Li, C.-T. Ng, L.-Y. L. Yung and B.-H. Bay, *Acta Pharmacol. Sin.*, 2011, **32**, 983.
20 S. Zeng, K.-T. Yong, I. Roy, X.-Q. Dinh, X. Yu and F. Luan, *Plasmonics*, 2011, **6**, 491.
21 D. A. Giljohann, D. S. Seferos, W. L. Daniel, M. D. Massich, P. C. Patel and C. A. Mirkin, *Angew. Chem., Int. Ed.*, 2010, **49**, 3280.
22 R. Sardar, A. M. Funston, P. Mulvaney and R. W. Murray, *Langmuir*, 2009, **25**, 13840.
23 A. Alizadeh, M. M. Khodaei, C. Karami, M. S. Workentin, M. Shamsipur and M. Sadeghi, *Nanotechnology*, 2010, **21**, 315503.
24 K.-W. Huang, C.-J. Yu and W.-L. Tseng, *Biosens. Bioelectron.*, 2010, **25**, 984.
25 H. Li, Q. Zheng and C. Han, *Analyst*, 2010, **135**, 1360.
26 W. Yang, J. J. Gooding, Z. He, Q. Li and G. Chen, *J. Nanosci. Nanotechnol.*, 2007, **7**, 712.
27 C.-C. Huang and H.-T. Chang, *Chem. Commun.*, 2007, 1215.
28 G. Wang, Z. Chen and L. Chen, *Progress in Chemistry*, 2010, **22**, 489.
29 G. Wang, Y. Wang, L. Chen and J. Choo, *Biosens. Bioelectron.*, 2010, **25**, 1859.
30 Y.-J. Lai and W.-L. Tseng, *Analyst*, 2011, **136**, 2712.
31 C.-Y. Lin, C.-J. Yu, Y.-H. Lin and W.-L. Tseng, *Anal. Chem.*, 2010, **82**, 6830.
32 Y.-Y. Chen, H.-T. Chang, Y.-C. Shiang, Y.-L. Hung, C.-K. Chiang and C.-C. Huang, *Anal. Chem.*, 2009, **81**, 9433.
33 Y.-L. Hung, T.-M. Hsiung, Y.-Y. Chen and C.-C. Huang, *Talanta*, 2010, **82**, 516.
34 G. Frens, *Nature-Physical Science*, 1973, **241**, 20.
35 J. B. Work, *Inorg. Synth.*, 1946, **2**, 221.
36 A. R. Murdock, T. Tyree and W. Otterbein, *Inorg. Chem.*, 1985, **24**, 3674.
37 R. C. Jin, G. S. Wu, Z. Li, C. A. Mirkin and G. C. Schatz, *J. Am. Chem. Soc.*, 2003, **125**, 1643.
38 G. Senanayake, *Gold Bull.*, 2005, **38**, 170.
39 G. Senanayake, *Miner. Eng.*, 2005, **18**, 995.
40 E. Molleman and D. Dreisinger, *Hydrometallurgy*, 2002, **66**, 1.
41 M. Gharehbaghi, F. Shemirani and M. D. Farahani, *J. Hazard. Mater.*, 2009, **165**, 1049.
42 R. Saavedra, C. Soto, J. Yanez and M. Ines Toral, *Microchem. J.*, 2011, **98**, 220.
43 V. Kaur, A. K. Malik and N. Verma, *J. Chin. Chem. Soc.*, 2007, **54**, 715.
44 C. Z. Huang, K. A. Li and S. Y. Tong, *Anal. Chim. Acta*, 1997, **345**, 235.